Spiral Orbit Tribometry — Part I: Description of the Tribometer

STEPHEN V. PEPPER
NASA-Glenn Research Center
Cleveland, Ohio 44135
and
EDWARD P. KINGSBURY
Interesting Rolling Contact
Walpole, Massachusetts 02081

A new rolling contact tribometer based on a planar thrust bearing geometry is described. The bearing "races" are flat plates that drive a ball into a near-circular, spiral path. The spiraling ball is returned to its initial radius each revolution around the race by a "guide plate" backed by a force transducer. The motions of the ball are analyzed and the force exerted by the ball on the guide plate is related to the friction coefficient of the system. The experimental characteristics of the system are presented and the system is shown to exhibit the behavior expected for a tribometer.

KEY WORDS

Bearings; Rolling Element; Ball; Boundary Lubrication; Engineering Analysis and Computing; Contact Mechanics; Friction; Boundary; Friction; Testing; Bench Tests

INTRODUCTION

Practical mechanical devices with moving parts generally require attention to their tribological properties – those parts of the mechanism that involve friction and wear and therefore usually require lubrication. Ball bearings are one of these devices and attention is given to the lubrication of the balls rolling in the races. Testing new lubricants and materials of construction for bearings is often done on the bearings themselves and even under the conditions and in the machine in which the bearing is to be incorporated. Such testing, while enjoying maximum credibility, can be very time-consuming and even impractical for operations intended to extend for many years.

In order to avoid the expense and time of full scale testing, instruments have been introduced that simplify and extract what is considered to be a crucial aspect of rolling bearing operation. Many of these "tribometers" are used to evaluate lubricants and bearing materials in abbreviated time and at smaller expense. Most of these instruments operate by sliding one element on another, with repeated passes over the same track, either circular or a short straight line. Direct application of the results to ball bearings is often questionable because some crucial aspect of the bearings operation, such as rolling, is lacking in these tribometers.

This report describes a new type of tribometer to test lubricants and materials in which the correspondence to the usual ball bearing motions is both close and evident. The elements of the tribometer– essentially a retainerless thrust bearing with one ball and flat races – is depicted in Fig.1. A ball, under load, is driven by the rotating plate into an orbit that is nearly circular. The orbit is, in fact, an opening spiral. At the end of an orbit the rolling ball contacts the "guide plate" and is guided back to the starting point

Final manuscript approved September 23, 2002
Review led by Tibor Tallian

NOMENCLATURE

h	= spiral pitch
F_{pg}	= force on the guide plate, normal to its face
F_1	= force on the ball at the contact with the rotating plate, normal to the guide plate's face. Considered here as the friction force
F_2	= force on the ball at the contact with the fixed plate, normal to the guide plate's face
$\boldsymbol{P}$	= Pivot, relative angular velocity between the ball and a plate
$\boldsymbol{r}$	= radius vector from ball's center to a point on its surface
R	= distance of ball's center from axis of rotating plate
$\boldsymbol{v}$	= velocity of a point on the ball's surface
$\boldsymbol{v}_r$	= velocity of the point of contact between the ball and the rotating plate
$\boldsymbol{v}_c$	= velocity of the ball's center
$\boldsymbol{V}$	= velocity of a point on the rotating plate's surface
ω	= angular velocity of the ball with respect to its center
Ω_p	= angular velocity of the rotating plate
Ω_o	= angular velocity of the ball's center about the axis of the rotating plate

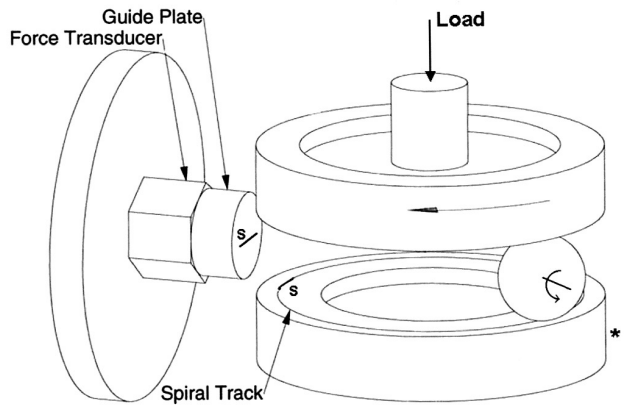

Fig. 1—Essential elements of the Spiral Orbit Tribometer. S denotes the scrub - that portion of the track made by the ball contacting the guide plate.

of the spiral, which then repeats. A force transducer attached to the guide plate senses the force developed during the guide plate's contact with the ball (termed the scrub, S) and it is this force that will be shown to be related to the friction force between the ball and the two large flat plates (races). The three plates, the ball and the force transducer are the elements of this Spiral Orbit Tribometer (SOT).

The authors kinematic analysis is first order, meaning that all elastic effects inside all Hertzian contacts are ignored. The single assumption of "roll without slip" then gives the kinematic relations between spin and orbit angular velocities outside the scrub (95% of an orbit). To first order inside the scrub the ball also rolls without slip on the fixed and guide plates, but, as will be shown, plain slip must occur between the ball and the rotating plate. This slip is completely independent of any elastic effects. It is radially inward on the rotating plate, and the force to produce it is measured by the force transducer behind the guide plate. It is this measurement that allows the friction coefficient to be determined by the SOT.

The spiral orbit is an essential feature of this tribometer. It is caused by pivot(spin)-induced tangential stresses within the Hertzian contacts between the ball and the plates, a second order effect called creep or micro-slip. Local displacements within the Hertzian contacts consist of elastic strain (stick) if the local tangential stress is less than the friction coefficient times the local normal pressure, and slip if it is greater. These micro-displacements integrate to give the lateral macro-displacements of the spiral. Johnson *(3)*, gives an encyclopedic account of micro-slip, including an account of the spiral. He notes, page 263, that "The difficulty of problems involving micro-slip lies in the different boundary conditions which have to be satisfied for the stick and slip zones [within a Hertzian contact] when the configuration of these zones is not known in advance." The spiral was first mentioned by Palmgren *(8)* and subsequently analyzed by Johnson *(1), (2)* and by Kalker *(4)*. The SOT spiral geometry without the force transducer was used by Kingsbury *(7)* to study lubricant degradation and the formation of friction polymer under boundary lubricated rolling conditions.

No attempt is made here to extend the analysis of the spiral. Instead it is simply accepted as a characteristic of the ball's motion and used as such in the operation of the tribometer. The pitch of the spiral turns out to be small enough - under an extremely wide range of conditions - to allow the ball to reach the guide plate's face without falling out or jamming against the side of the guide plate. The spiral has always been present in the many versions of this device that have been constructed and it has been found to be an exceedingly robust phenomenon on which the operation of the tribometer can depend.

The motions of the ball are analyzed in Section II. The analysis explains how the coefficient of friction is obtained from the force experienced by the guide plate, thus earning the name "tribometer" for this device. The experimental behavior of the tribometer and observations that support rather general aspects of the analysis are given in Section III. Some attention is also given to the correspondence between the present experimental results and the analysis and earlier experimental observations of Johnson *(1)* with three symmetrically spaced balls, instead of the single ball used in the present configuration.

ANALYSIS

The purpose of the analysis is to understand the motion of the ball, both in and out of the scrub, and the means by which this instrument measures the coefficient of friction. To do so requires obtaining expressions for the angular velocity of the ball in both regions. This analysis indicates the locus of slip between the ball and plates and ultimately indicates the relationship between the coefficient of friction and the force experienced by the guide plate. The analysis is based on roll without slip between rigid bodies, which means that there is no relative linear velocity at the ball-plate contact. The reason for this requirement is that rolling friction is an order of magnitude smaller than sliding friction, even for the most favorable boundary lubricated conditions. The condition of roll without slip can be satisfied at all contacts in the system except for the contact of the ball on the rotating plate in the scrub region - this contact exhibits gross sliding. The spiral itself is not treated explicitly in the following analysis because those aspects of the ball's motion that lead to the device's operation as a tribometer can be understood without doing so. The analysis will first treat the motion outside the scrub followed by the motion in the scrub.

Outside the Scrub

The following analysis is so elementary that the results are often quoted without proof *(1)*. The value of the detail shown here is that it provides the framework for the analysis of the motion in the scrub. The goal here is to obtain an expression for the ball's angular velocity.

The velocity of a point on the ball's surface, $\mathbf{v}(\mathbf{r})$, is given by

$$\mathbf{v}(\mathbf{r}) = \mathbf{v}_c + \omega x \mathbf{r} \qquad [1]$$

where $\mathbf{r}$ is the radius vector from the ball's center to any point on its surface, ω is the angular velocity of the ball and $\mathbf{v}_c$ is the veloc-

ity of the ball's center. Boldface denotes vectors. If $\mathbf{r}_b$ is the radius vector from the ball center to the rotating plate contact, the velocity of the ball at this contact, $\mathbf{v}_r$, is

$$\mathbf{v}_r = \mathbf{v}_c + \omega x \mathbf{r}_b \quad [2]$$

If **V** is the velocity vector of the rotating plate at the point of contact, roll without slip requires $\mathbf{V} = \mathbf{v}_r$, so:

$$\mathbf{V} = \mathbf{v}_c + \omega x \mathbf{r}_b \quad [3]$$

For the contact at the fixed plate, $\mathbf{r} = -\mathbf{r}_b$, and roll without slip requires

$$0 = \mathbf{v}_c - \omega x \mathbf{r}_b \quad [4]$$

Adding Eqs. [3] and [4] yields

$$\mathbf{v}_c = \frac{\mathbf{V}}{\mathbf{2}} \quad [5]$$

This vector relation indicates that the ball is driven in the direction of the rotating plate velocity vector at the contact. The rotating plate drives the ball in a circular orbit, a consequence of roll without slip. Also, Ω_O, the orbital angular velocity of the ball center, and Ω_p, the plate rotation rate, are related as

$$\Omega_o = \frac{\Omega_o}{2} \quad [6]$$

The ball center orbit rate is thus half the rotating plate's rotation rate. This relationship is independent of the ball radius r_b and the radius of the (nearly) circular track, R.

The angular velocity of the ball, ω, can now be determined by referring to Fig. 2. First, subtracting Eq. [4] from Eq. [3] yields

$$\mathbf{V} = 2\omega x \mathbf{r}_b \quad [7]$$

By choosing different directions of the vector $\mathbf{r}_b$, Eq. [7] can be used to determine the components of the vector ω. With the ball in the position shown and $\mathbf{r}_b = r_b\mathbf{k}$, $\mathbf{V} = \Omega_p R\mathbf{i}$, and $\omega = \omega_I\mathbf{i} + \omega_j\mathbf{j} + \omega_k\mathbf{k}$, substituting into Eq. [7] yields

$$\Omega_p R\mathbf{i} = 2r_b(-w_i\mathbf{j} + \omega_j\mathbf{i}) \quad [8]$$

So that the relations on rolling balls found in elementary texts are

$$\omega_I = 0 \quad \text{and} \quad \omega_j = \frac{\Omega_p R}{2r_b} \quad [9]$$

To find the third component of ω, let $\mathbf{r} = r_b\mathbf{j}$, the point on the ball furthest from the k axis. The velocity of this point must be $\Omega_o(R+r_b)$ in the **i** direction. Then using Eq. [1],

$$\Omega_o(R+r_b)\mathbf{i} = \Omega_o R\mathbf{i} + (\omega_j\mathbf{j} + \omega_k\mathbf{k}) \times r_b\mathbf{j} \quad [10]$$

which leads to

$$\omega_k = -\Omega_o = -\Omega_p/2 \quad [11]$$

The complete angular velocity vector of the ball at the position shown is thus

$$\omega = \frac{\Omega_p R}{2r_b}\mathbf{j} - \frac{\mathbf{\Omega_P}}{\mathbf{2}}\mathbf{k} \quad [12]$$

The ball thus undergoes one complete rotation about its own vertical axis for each circular orbit so that the locus of points of contact on its surface is a great circle. Two means by which the rest of the ball's surface – and any lubricant there – can be brought into contact are described below.

The difference between the **k** component of the ball's angular velocity and the angular velocity of the contacting plate - their relative angular velocity – is referred to here as pivot and as spin by Johnson *(1)*. For the contact at the rotating plate,

$$\mathbf{P_r} = -\frac{\mathbf{\Omega_P}}{\mathbf{2}}\mathbf{k} \quad [13a]$$

And for the contact at the fixed plate,

$$\mathbf{P_f} = +\frac{\mathbf{\Omega_P}}{\mathbf{2}}\mathbf{k} \quad [13b]$$

The significance of pivot is that it gives rise to sliding and frictionally-induced energy loss within the Hertzian contact area of elastic bodies under load. This energy dissipation within the pivoting contact can be considered a driving force for the degradation of liquid lubricants. Note that pivot and its associated energy loss are absent for a ball rolling in a straight line, even for elastic materials with non-zero Hertzian contact area.

The kinematics of the retainerless thrust bearing described here and an angular contact bearing are related in that both exhibit pivot *(5), (6)*. The sum of the absolute pivots for the thrust bearing is Ω_p and it has a contact angle of π/2. According to first order kinematic formulas for angular contact bearings, the sum of the absolute pivots for any bearing in any rotational mode is its total speed times the sine of the contact angle. This relationship also holds for this thrust bearing and establishes its connection to those bearings with curved surfaces that also exhibit pivot.

Referring to Fig.2, the spiral can be described as the result of a nonzero **i**-component of ω. This component moves the locus of contact on the ball off the great circle it would have if the orbit was a perfect circle and instead generates a spiral on the ball as it rolls in its spiral orbit. This has the beneficial effect of continuously bringing new lubricant into the contacts from parts of the ball other than the great circle associated with a perfectly circular orbit. Another way that the ball's entire surface is exercised will be indicated in the following discussion of motion in the scrub.

In The Scrub

The ball now has three simultaneous contacts: rotating plate, fixed plate and guide plate. The analysis seeks the ball's linear velocity, $\mathbf{v}_c$, and angular velocity, ω, subject to the requirement that there be roll without slip if possible. In Fig. 3, the scrub is depicted as it appears on the fixed plate where the angle included by the scrub is denoted by θ_{max}. The linear velocity of the ball's center is denoted by $|\mathbf{v}_c(\theta)|\mathbf{i}$, where the θ-dependence indicates that $|\mathbf{v}_c|$may vary within the scrub. Now let $\omega = \omega_I\mathbf{i} + \omega_j\mathbf{j} + \omega_k\mathbf{k}$ and treat the contact with the bottom plate, $\mathbf{r} = -r_b\mathbf{k}$. The velocity

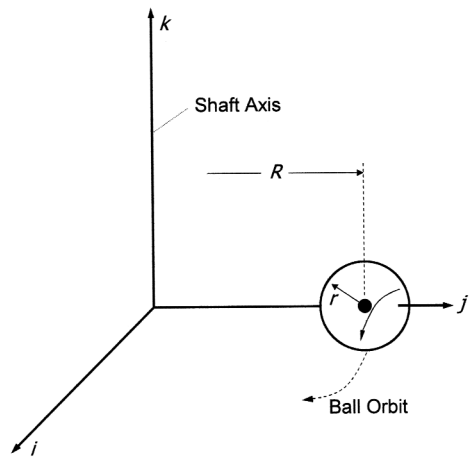

Fig. 2—Coordinate system used to analyze ball motion our of the scrub region.

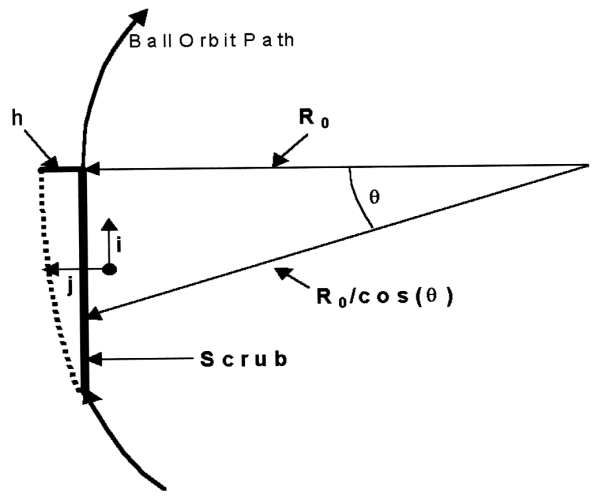

Fig. 3—Ball path and coordinate system on fixed plate around scrub region.

at this point must be zero for roll without slip, so using Eq. [1],

$$0 = |\mathbf{v}_c(\theta)|\mathbf{i} + \omega x(-r_b\mathbf{k}) = [|\mathbf{v}_c(\theta)|-r_b\omega_j]\mathbf{i} + r_b w_I\mathbf{j} \quad [14]$$

Therefore

$$\omega_I = 0 \qquad \text{and} \qquad \omega_j = \frac{|\mathbf{v_c}(\theta)|}{\mathbf{r_b}} \quad [15]$$

and roll without slip is possible at this contact. For the contact with the guide plate, $\mathbf{r} = r_b\mathbf{j}$, and roll without slip demands that

$$0 = |\mathbf{v}_c(\theta)|\mathbf{i} + [\{|\mathbf{v}_c(\theta)|/r_b\}\mathbf{j} + \omega_k\mathbf{k}] \times r_b\mathbf{j} = [|\mathbf{v}_c(\theta)| - \omega_k r_b]\mathbf{i} \quad [16]$$

So that

$$\omega_k = \frac{|\mathbf{v_c}(\theta)|}{\mathbf{r_b}} \quad [17]$$

The ball rolls without slip simultaneously on the fixed plate and on the guide plate. The complete angular velocity vector for the ball in the scrub is

$$\omega = \frac{|\mathbf{v_c}(\theta)|}{\mathbf{r_b}}(\mathbf{j} + \mathbf{k}) \quad [18]$$

Now $|\mathbf{v}_c(\theta)|$ is determined by considering the contact at the rotating plate, $\mathbf{r} = r_b\mathbf{k}$. From Fig. 3, the velocity of the rotating plate at the contact is

$$\mathbf{V} = \frac{\Omega_p \mathbf{R_o}}{\cos(\theta)}[\cos(\theta)\mathbf{i} + \sin(\theta)\mathbf{j}] = \Omega_p\mathbf{R_o}[\mathbf{i} + \tan(\theta)\mathbf{j}] \quad [19]$$

The velocity of the ball surface at this contact is

$$\mathbf{v} = |\mathbf{v_c}(\theta)|\mathbf{i} + \frac{|\mathbf{v_c}(\theta)|}{\mathbf{r_b}}(\mathbf{j} + \mathbf{k}) x \mathbf{r_b}\mathbf{k} = \mathbf{2}|\mathbf{v_c}(\theta)|\mathbf{i} \quad [20]$$

The relative velocity at this contact is then

$$\Delta\mathbf{V} \equiv \mathbf{V} - \mathbf{v} = [\Omega_p R_o - 2|\mathbf{v}_c(\theta)|]\mathbf{i} + \Omega_p R_o \tan(\theta)\mathbf{j} \quad [21]$$

Roll without slip is possible for the **i**-component of relative velocity if

$$|\mathbf{v_c}(\theta)| = \frac{\Omega_p \mathbf{R_o}}{\mathbf{2}} \quad [22]$$

which determines the velocity of the ball center in the scrub as being independent of its position in the scrub and the same as the velocity outside the scrub. The complete angular velocity vector of the ball in the scrub can now be written as

$$\omega = \frac{\Omega_p R_o}{2r_b}(\mathbf{j} + \mathbf{k}) \quad [23]$$

Although the **i**-component of relative velocity at the rotating plate contact can be zero, the **j**-component is not zero. There is slip at this contact with a relative sliding velocity normal to the guide plate of

$$\Delta\mathbf{V} = \Omega_p R_o \tan(\theta)\mathbf{j} \quad [24]$$

This gross slip (that is to say slip over the whole of the Hertzian contact area between the ball and the rotating plate) occurs only by the ball in the scrub sliding on the rotating plate, with the direction of the slip normal to the guide plate. The slip velocity depends on the ball's position in the scrub via the dependence of $\Delta\mathbf{V}$ on θ.

This slip at the ball – rotating plate interface generates a friction force that must in turn generate a reaction force on the guide plate and also possibly on the fixed plate. In order to understand these friction and reaction forces and to see how the guide plate force can yield a coefficient of friction, refer to Fig. 4, where the lateral forces on the ball are depicted. The friction force of the rotating plate sliding on the ball in the scrub is denoted as F_1, the reaction force of the guide plate is denoted as F_{gp}, and F_2 is the force included to accommodate the possibility that there is a lateral force on the ball at the contact with the fixed plate. The relationship between these forces is determined by the requirement that the sum of these lateral forces is zero and that the sum of their

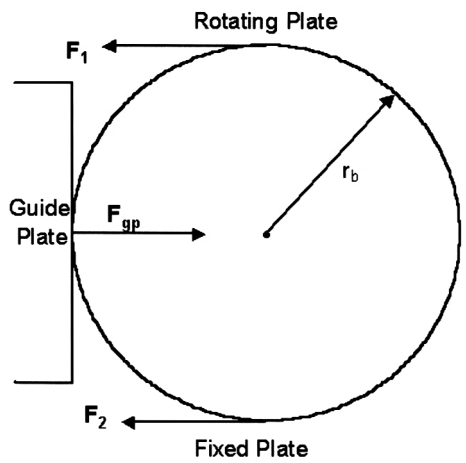

Fig. 4—Lateral forces on the ball in the scrub.

moments is zero. Summing the moments around the ball center yields

$$F_1 r_b = F_2 r_b \quad \Rightarrow \quad F_1 = F_2 \qquad [25a]$$

Summing the lateral forces yields

$$F_{gp} = F_1 + F_2 = 2F_1 \qquad [25b]$$

There are two consequences of Eqs. [25]. (1) The guide plate force is twice the friction force at the sliding contact with the rotating plate. This establishes the ability of this thrust bearing device to measure the friction force by the transducer on which the guide plate is mounted and the coefficient of friction (CoF) by dividing this friction force by the load:

$$CoF = \frac{F_{gp}}{2 \times load} \qquad [26]$$

The friction is measured only during ~ 5% of the orbit traversed by the ball. (2) There is a lateral force on the ball at the contact with the fixed plate and an associated reaction force on the fixed plate itself, trying to push the fixed plate away from the guide plate. Experimental confirmation of this force on the fixed plate, normal to the guide plate, will be indicated in Section III. There may also be forces on all the elements that are tangential to the guide plate's face, i.e. in the **i** - direction. However, the force transducer only senses forces in the **j**-direction, so that forces tangential to the guide plate's face are not considered further here.

The expressions for the pivot at the three contacts of the ball in the scrub can be obtained from Eq. [23]. For the contact with the fixed plate,

$$\mathbf{P_f} = -\frac{\mathbf{\Omega_p R_o}}{\mathbf{2 r_b}}\mathbf{k} \qquad [27a]$$

For the guide plate contact,

$$\mathbf{P_{gp}} = -\frac{\mathbf{\Omega_p R_o}}{\mathbf{2 r_b}}\mathbf{j} \qquad [27b]$$

For the contact with the rotating plate,

$$\mathbf{P_r} = -\mathbf{\Omega_p}(\mathbf{1} + \frac{\mathbf{R_o}}{\mathbf{2 r_b}})\mathbf{k} \qquad [27c]$$

The values of these pivots are greater than those outside the scrub (Eqs. [13]) by a factor R_o/r_b (≈4 in the experimental system to be described below). These relative angular velocities cause interfacial slip in the elastic contact areas in the same way as that for the ball moving outside the scrub and have experimentally observable consequences as discussed in Sec. III.

The analysis shows that the **k** component of angular velocity, due to the ball rolling on the guide plate, rotates the ball off the spiral of contact it had upon entering the scrub and thus generates new spirals of contact on the ball each time it passes through the scrub. This allows the entire surface of the ball to eventually be brought into contact with the plates and its associated lubricant to be stressed. This motion is different from that of the usual ball-on-flat sliding configuration in which the same spot on the ball is continuously slid upon, generating a flat wear scar. No such wear scar on the ball is developed by this spiral orbit tribometer. Thus a sphere on flat geometry is maintained throughout the operation of this tribometer and simple formulas for elastic solids can be used for the area of contact and pressure within the contact.

The approach to tribometry presented here is certainly unconventional. It is thus desirable to compare the CoFs obtained with the SOT (using Eq. [26]) with CoFs obtained by more conventional methods. Such a comparison will be made in the next section and, where possible, in subsequent publications.

EXPERIMENTAL CHARACTERIZATION

The experimental system described here was constructed with rotating and fixed plates 50.8 mm (2 in) diameter, a guide plate 12.7 mm (.5 in) diameter and ball diameters of both 6.35 mm (.25 in) and 12.7 mm (.5 in). The ball's orbit diameter was about 45.72 mm (1.8 in). The operational environment could be ultrahigh vacuum or selected gases at atmospheric pressure, all at room temperature.

Some general observations support the above analysis. The ball's orbit is very close to circular, in accord with Eq. [5], a consequence of roll without slip. Also from Eq. [5], the ball's angular velocity should be half that of the rotating plate. This was tested by simply counting both the number of ball orbits and the number of plate rotations over many orbits. This was maintained at 1:2 over many hundreds, even thousands of orbits, in accord with the analysis. Eventually, however, the number of ball orbits fell behind the predicted value so that the ball orbit rate had been slightly less than half the rate of the rotating plate from the start. This "velocity deficit" of the ball has been noted and explored somewhat further in an earlier report *(9)* on the tribometer's development. It is really a small second order effect that can generally be ignored in the usual operation of the tribometer as a lubricant tester. It does, however, play a role on the appearance of the marks made by the ball on the rotating plate, as explained below.

A micrograph of the scrub region on the fixed plate is shown in Fig. 5 for a system load of 1.5 GPa. Circular arcs are apparent in the degraded lubricant. These scars are due to the rotation of the 12.7 mm diameter ball about the **k** axis while rolling on the guide

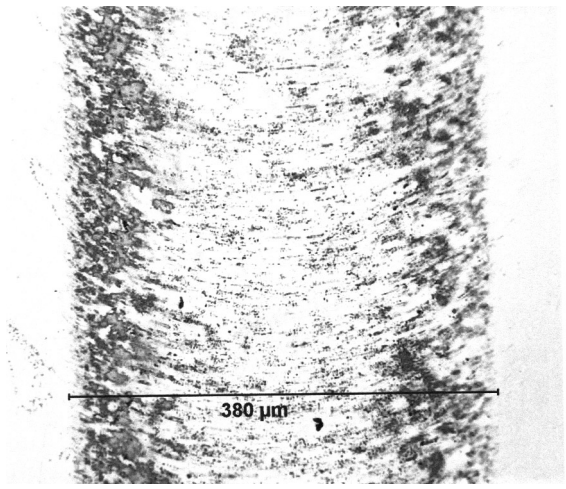

Fig. 5—Micrograph of scrub region on steel fixed plate after ~1000 orbits under 43 lb. Load.

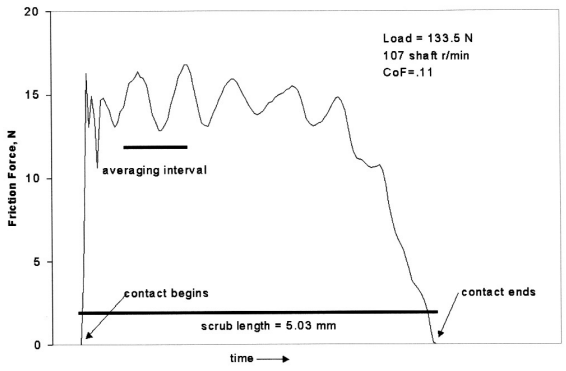

Fig. 6—Typical force profile.

plate, as explained below Eqs. [27]. There are corresponding scars on the guide plate due to the ball rolling about the **j** axis while rolling on the fixed plate. These scars can be regarded as experimental support for the analysis that lead to Eqs. [27a] and [27b]. The track width on the fixed plate is quite close to the Hertz value of 0.4 mm.

A corresponding scar on the rotating plate is predicted by Eq. [27c]. Such a scar should appear on only one place on the rotating plate because, according to the simple theory, the ball should enter the scrub at the same place on the rotating plate at each orbit. However, the velocity deficit noted above slightly changes this place on the rotating plate each successive orbit, so that a series of circular arc scars eventually is established around the track. This is the most easily observable consequence of the velocity deficit, which also has the effect of "spreading out" the scrub region on the rotating plate so that eventually friction is measured all around its track. The circular arc scars are not found outside the scrub on the fixed plate because the pivot value there, Eq. [13b], is too small for the scars to be observable.

An important result of the analysis is that a lateral force $F_2 = F_{gp}/2$ is developed at the fixed plate contact, with the reaction force pushing the fixed plate away from the guide plate. This was tested by supporting the fixed plate on rollers, allowing free motion normal to the guide plate, and constraining its motion by a second force transducer placed at the asterisk in Fig. 1. Both the guide plate force F_{gp} and the lateral force F_2 on the fixed plate were then measured simultaneously. It was found that $F_2 = F_{gp}/2$ very closely. This important experimental validation of the analysis thus provides confidence in the identification of $F_{gp}/2$ with the friction force F_1 and permits the identification of this device as a "tribometer."

To obtain the coefficient of friction (CoF) in this tribometer, the guide plate force obtained by a digital data acquisition system is divided by 2 to obtain the friction force and by the load to obtain the CoF. The length of the scrub – the distance in which the ball is in contact with the guide plate – is obtained from the data acquisition rate and the linear velocity of the ball, Eq. [22]. A typical "force profile" is shown in Fig. 6. There is a sharp increase in the friction force, followed by oscillations. An average value of the friction force, obtained over the indicated interval, is divided by the load to obtain the CoF. The magnitude of these oscillations depend on the ball velocity. They are virtually absent for plate speeds < 60 r/min and become more evident at higher speeds. However, in spite of these oscillations, the CoF was found to be independent of speed for many material combinations as long as the friction force is averaged over an appropriate interval as shown. The oscillations appear to be due to a dynamic "ringing" response of the rotating shaft or other parts of the support structure. They are thus specific to this particular construction and may not appear in other versions. Their presence is not a severe drawback to the operation of this tribometer as long as the averaging is performed as indicated. A demonstration of this was obtained by stopping a test in mid-run, replacing a steel washer between the guide plate and the force transducer with a "soft" o-ring, and restarting. Oscillations were suppressed, but the same friction coefficient was obtained from the averaging software for both steel and o-ring configurations.

A demonstration of this device's ability to perform as a tribometer is its ability to demonstrate Amonton's Law, the independence of CoF on load. While not all physical systems actually do obey Amonton's Law, it has been found that it can be demonstrated in this tribometer with steel specimens running in the boundary lubricated regime. Figure 7 shows the results on the CoF of stepping up the load about every 100 orbits. The independence of CoF~.11 on load is evidently obeyed well over this load range, raising confidence in the operation of this device as a tribometer. Note also the impressive orbit to orbit reproducibility of the CoF. This demonstrates the effectiveness of the above averaging procedure in dealing with the oscillations in the force profile. Also note that a value of .11 for the CoF is reasonable for boundary-lubricated steel running in air. Referring here to the points raised at the end of Section II, this demonstration of Amonton's Law and the reasonableness of the CoF is experimental support for the basic result of the analysis – that the CoF can be obtained from half the guide plate force divided by the load.

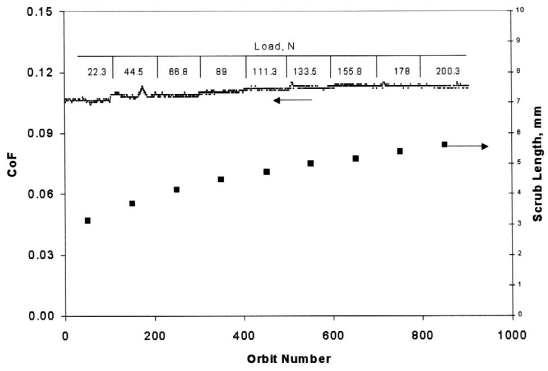

Fig. 7—The effect of varying load on CoF and scrub length for a boundary lubricated system running in air.

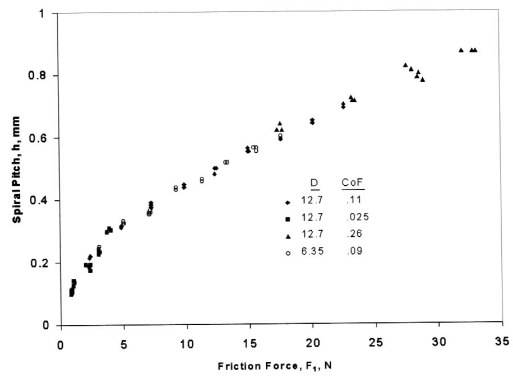

Fig. 9—The spiral pitch *vs.* friction force for different conditions.

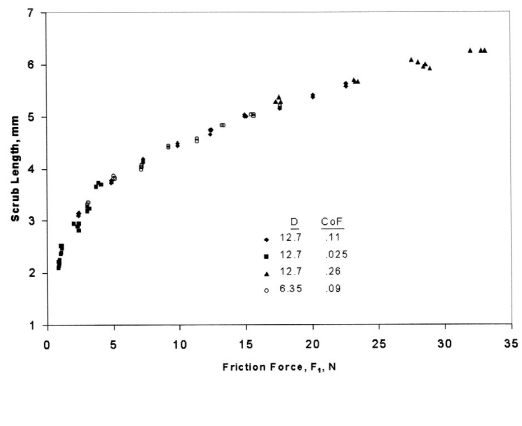

Fig. 8—Scrub length *vs.* friction force for different conditions. D is the ball diameter (mm).

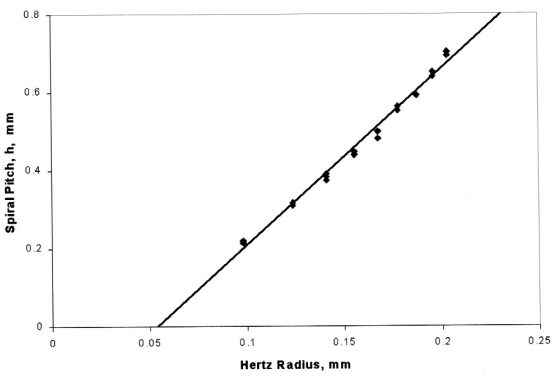

Fig. 10—Spiral pitch *vs.* Hertz radius.

The scrub length is also plotted in Fig. 7. Although it increases with load, this increase could just as well be ascribed to the increase in friction force as the load increases. To determine the dependence of scrub length on system parameters, the data for scrub length plotted in Fig. 8 was collected. From this it appears that the scrub length is determined only by friction force and not by CoF or load. This plot serves as a characterization of this system and shows that the scrub can be accommodated by the 12.7 mm (.5 in) diameter guide plate for a wide range of conditions, a characteristic that imparts important generality to this tribometer. The spiral itself, as well as the scrub, can be characterized for this system. The spiral's pitch, h (growth of the spiral's radius per orbit), can be obtained from the scrub length via Fig. 3 as

$$\mathbf{h = 2\pi R_o \frac{\sqrt{x^2+1}-1}{2\pi - atan(x)}} \qquad [28]$$

where R_o is the spiral's initial radius and x = scrub length / R_o. The data from Fig. 8 is used to plot the spiral's pitch in Fig. 9. The pitch is less than 1 mm for the conditions explored, which further characterizes this tribometer.

This section is concluded by considering the closely related earlier work of Johnson *(1)*. His analysis of the contact conditions of this kind of thrust bearing lead him to propose that the spiral's pitch (he calls it creep) is proportional to the radius of the circle of elastic contact (Hertz radius). This proposal was tested for the present arrangement by plotting in Fig. 10 the pitch for the data set associated with Fig. 7 *vs*. the Hertz radius. A straight line has been placed through the data points and the fit to linearity is observed to be fairly good. However, this linear fit does not extrapolate to the origin. Instead, for Hertz radii <.06 mm (<1 lb. load), the extrapolation implies negative values for the spiral's pitch. Such inward-going spirals have never been observed. Johnson's experimentally observed pitches did extrapolate to the origin. Thus, although the value of the pitch is roughly the same in both studies, the data presented here are not in full accord with Johnson's results. The reason for the lack of full accord may be that some aspects of the present system do not conform to the conditions met in Johnson's work. In particular, the use of one ball instead of Johnson's three symmetrically spaced balls may introduce an asymmetry not accounted for in the analysis. Although the present system was constructed as a tribometer to test lubricants and not as a means to test theories of the spiral, such theories provide insight to the slip conditions in the contact where the lubricant is degraded. Understanding these slip conditions may lead to better

understanding the details of boundary lubrication and tribochemical degradation of lubricants.

CONCLUSIONS

A new rolling contact tribometer based on a planar thrust bearing geometry has been described. It is a tribometer by virtue of its ability to measure a coefficient of friction. Except possibly in the region of the scrub, the first order kinematics of the instrument are well understood and are directly related to those of angular contact ball bearings. The flat race geometry lends itself to easy post-test examination of the tracks established by the passage of the ball. The open geometry of the instrument can accommodate in-situ analytic probes to investigate changes in surface chemistry. The lack of significant specimen wear allows the use of simple equations of sphere on flat geometry for pressure and contact area. The instrument has been operated in both ultrahigh vacuum and ambient pressure environments.

The analysis of the contact identified two loci of slip: the first is the slip within the elastic region of contact due to pivot - the relative angular velocity normal to the ball's plane of contact as it rolls on the plates. This type of slip is present in angular contact ball bearings and provides the most direct correspondence of this simpler system's kinematics with those of the typical ball bearing. The other type of slip, gross sliding, occurs between the ball and the rotating plate when the ball is in contact with the guide plate. It may be likened to the sliding of a ball against the pocket of a retainer in the usual ball bearing. The guide plate in this system may also be considered a retainer of sorts in that it keeps the ball from falling out of the system. The frictional energy loss that occurs in both regions of slip may be considered a driving agent for the degradation of organic lubricants within the contact.

This device, the SOT, simplifies a ball bearing down to irreducible elements – a single ball under load rolling on flat plates – and yet it manifestly *is* a ball bearing. As such, the results obtained with it on lubricant behavior should be directly applicable to the lubricant when used in the usual angular contact ball bearing. A following paper (Part II) reports the results of a study of the relative tribo-degradation rate of liquid lubricants in ultrahigh vacuum using the spiral orbit tribometer. Subsequent papers will report on using this technique to study friction polymer generation and solid film lubricants.

ACKNOWLEDGMENT

The authors wish to thank Professor Thierry Blanchet, Rensselaer Polytechnic Institute, for critical comments.

REFERENCES

(1) Johnson, K. L. (1958), "The Effect of Spin Upon the Rolling Motion of an Elastic Sphere on a Plane," *Jour. Applied Mech., Trans. ASME,* **25**, pp 332-338.

(2) Johnson, K. L. (1959), "The Influence of Elastic Deformation Upon The Motion of a Ball Rolling Between Two Surfaces," in *Proc. Inst. Mech. Engrs.,* **173**, 34, pp 795-810.

(3) Johnson, K. L. (1987), *Contact Mechanics*, Cambridge University Press, Cambridge, UK. Paperback Edition (with corrections), reprinted 1994.

(4) Kalker, J. J. (1990), *Three Dimensional Elastic Bodies in Rolling Contact*, Kluwer Academic Publishers, Dordrecht, The Netherlands, Sec. 5.2.2.

(5) Kingsbury, E. P. (1984), "Pivoting and Slip in an Angular Contact Bearing," *ASLE Trans.*, **27**, pp 259-262.

(6) Kingsbury, E. P. (1985), "First Order Ball Bearing Kinematics," *ASLE Trans.*, **28**, pp 239-243.

(7) Kingsbury, E. P. (1989), "Tribology in Slow Rolling Bearings," *Mat. Res. Soc. Symp. Proc.*, **140**, pp 437-442.

(8) Palmgren, P. (1928), "Investigations With Regard to Rolling Under Tangential Pressure," *Ball Bearing Journal*, 3, S.K.F. Company.

(9) Pepper, S. V., Kingsbury, E. P. and Ebihara, B. T. (1996), "A Rolling Element Tribometer for the Study of Liquid Lubricants in Vacuum," **NASA TP 3629**, NASA, Cleveland, OH.